Bioorganic & Medicinal Chemistry Letters 18 (2008) 4442–4446

Contents lists available at ScienceDirect

Bioorganic & Medicinal Chemistry Letters

journal homepage: www.elsevier.com/locate/bmcl

Imidazole piperazines: SAR and development of a potent class of cyclin-dependent kinase inhibitors with a novel binding mode

M. Raymond V. Finlay [a,*], David G. Acton [a], David M. Andrews [a], Andrew J. Barker [a], Michael Dennis [a], Eric Fisher [a], Mark A. Graham [a], Clive P. Green [a], David W. Heaton [a], Galith Karoutchi [a], Sarah A. Loddick [a], Rémy Morgentin [c], Andrew Roberts [a], Julie A. Tucker [b], Hazel M. Weir [a]

[a] Cancer and Infection Research Area, AstraZeneca Pharmaceuticals, Alderley Park, Macclesfield, Cheshire SK10 4TG, UK
[b] Lead Generation Discovery Enabling Capabilities and Sciences, AstraZeneca Pharmaceuticals, Alderley Park, Macclesfield, Cheshire SK10 4TG, UK
[c] AstraZeneca Research Unit, Chemin de Vrilly, Z.I. la Pompelle BP 1050, 51689 Reims Cedex 2, France

ARTICLE INFO

Article history:
Received 29 April 2008
Revised 6 June 2008
Accepted 6 June 2008
Available online 12 June 2008

Keywords:
CDK
Kinase
Inhibitor
Cancer

ABSTRACT

A piperazine series of cyclin-dependent kinase (CDK) inhibitors have been identified. The compounds exhibit excellent physiochemical properties and a novel binding mode, whereby a bridging interaction via a water molecule with Asp 86 of CDK2, leads to selectivity for the CDK family of enzymes over other kinases. Piperazines **2e** and **2i** were subsequently shown to inhibit tumour growth when dosed orally in a nude mouse xenograft study. Additional chemical series that exploit this unexpected interaction with Asp 86 are also described.

In a previous letter,[1] we described the development of a series of novel imidazole-substituted CDK inhibitors. To further explore SAR within this area, we decided to examine alternative substituents to the previously described sulfonamides and sulfones at the 4-position of the aniline ring (Table 1).

Whilst these changes led to the identification of a number of potent CDK2 inhibitors (i.e., **1a** and **1e**), these compounds demonstrated a number of suboptimal properties during initial screening. These included cytochrome P450 inhibition, high levels of serum protein-binding and affinity for the hERG ion channel (data not shown). Acquired long-QT syndrome causes significant cardiac side effects and represents a major problem in clinical studies of drug candidates. One of the reasons for development of arrhythmias related to long QT is inhibition of the human ether-a-go-go-related-gene (hERG) potassium channel.[2] Therefore, early identification of hERG affinity is becoming increasingly important. We thus chose to profile the compounds early in the cascade using a high-throughput patch-clamp hERG assay.[3] In addition, P450 inhibition by a CDK inhibitor raises the concern of possible drug interactions resulting from abrogation of the P450 pathway(s) of metabolism, and causing toxicity due to elevated exposures to other drugs metabolized by these pathways.

Table 1
Structures and in vitro activity for imidazoles **1** and **2**

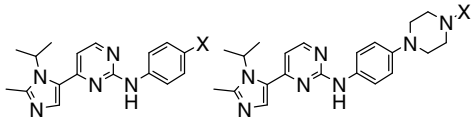

1 **2**

Compound	X	CDK2 IC_{50} (μM)	MCF-7 proliferation IC_{50} (μM)
1a	CN	<0.003	0.07
1b	NMe_2	0.024	0.068
1c	OMe	0.008	—
1d	F	0.003	0.100
1e	Cl	<0.003	—
1f	$SO_2NHCH_2CH_2OMe$	<0.003	0.045
2a	SO_2CH_3	0.032	0.072
2b	$COCH_3$	<0.003	0.145

Most of the properties described above could be attributed to the relatively high lipophilicity of these compounds. The less lipophilic piperazine series (**2**), however, appeared to be potent and devoid of the above issues, and we elected to further explore this class of inhibitor.

* Corresponding author. Tel.: +44 1625 510379.
E-mail address: ray.finlay@astrazeneca.com (M. Raymond V. Finlay).

0960-894X/$ - see front matter © 2008 Elsevier Ltd. All rights reserved.
doi:10.1016/j.bmcl.2008.06.027

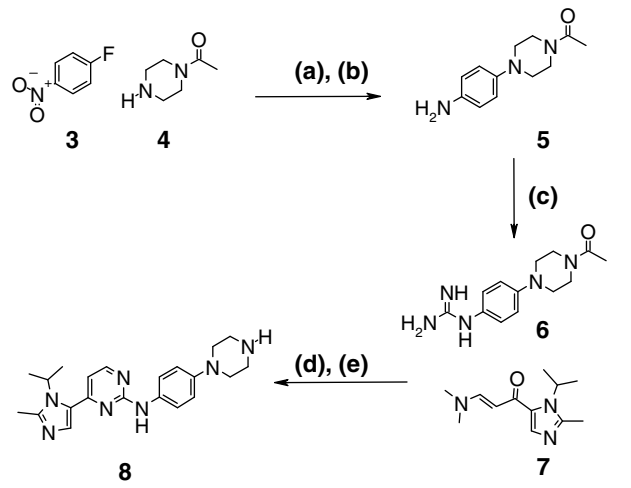

Scheme 1. Synthesis of piperazine intermediate **8**. Reagents and conditions: (a) K_2CO_3, NMP, 120 °C, 2 h, 80%; (b) H_2 gas, 10% Pd/C, EtOH, 99%; (c) $NCNH_2$, HCl, Dioxane, EtOH, 90 °C, 30 h, 70%; (d) 2-Methoxyethanol, 110 °C, 75%; (e) concd HCl, *iso*-propanol, 28%.

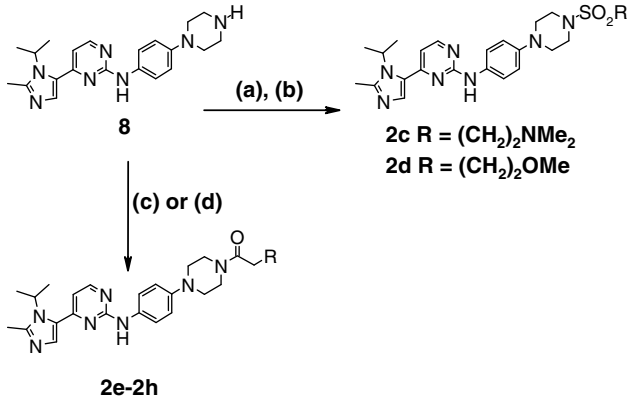

Scheme 2. Synthesis of piperazine amides and sulfonamides **2**. Reagents: (a) $ClSO_2CH_2CH_2Cl$, Et_3N, CH_2Cl_2, 31%; (b) NMe_2, THF, 80%, or NaOMe, Methanol, 28%; (c) Carboxylic acid, HATU, DIPEA, DMF, 20–95%; (d) i—chloroacetyl chloride *i*-Pr_2EtN, CH_2Cl_2, 87%; ii—amine, THF, 80–90%.

The piperazines were prepared using a modification to the route described by us previously[1] (Scheme 1).

Thus, 4-fluoro-nitrobenzene (**3**) was coupled with 1-acetyl-piperazine (**4**) under basic conditions. Following reduction of the nitro group, the resulting aniline **5** was reacted with cyanamide to produce guanidine **6** as the bicarbonate salt. Cyclisation with the known aminopropenone **7** followed by hydrolysis gave the piperazine **8**. Further reaction with 2-chloro-1-ethanesulfonyl chloride followed by in situ elimination gave the vinyl sulfonamide. This could undergo conjugate addition with both sodium methoxide and dimethylamine to give **2c** and **2d**, respectively (Scheme 2).

Methyl sulfonamide **2a** was prepared in a slightly different way as shown in Scheme 3. Reaction of guanidine with aminopropenone **7** gave the amino pyrimidine **9**. Buchwald coupling[4] with bromo compound **11** (derived from sulfonylation of commercial piperazine **10**) then provided the required compound **2a**.

Although the piperazine sulfonamides displayed good cell and enzyme potency[6] (Table 2), the aqueous solubility of the neutral sulfonamides was less than 20 μM, possibly driven by their moderate lipophilicity (Log*D* between **2** and **3**), and we elected to explore the piperazinyl amide series to see if this property could be modulated.

Mindful of the solubility properties of the sulfonamides, a number of basic and hydrophilic amides were targeted. The latter were prepared by coupling with activated carboxylic acids (e.g., glycolic acid or *S*-lactic acid) leading to amides **2e**[5] and **2f** (Scheme 2).

Basic amides (**2g** and **2h**) were accessed by reaction with chloro-acetyl chloride followed by displacement with dimethylamine or diethylamine. We were pleased to observe that once more the compounds displayed good levels of enzyme and cell potency (Table 2), and in general manifested acceptable physical properties.

Clearly, a reduction in Log*D* benefits aqueous solubility (cf. **2a** and **2e**) although in the case of **2e** (Log*D* = 1.7 and solubility = 160) and **2f** (Log*D* = 2.2 and solubility = 370), we anticipate that the presence of the chiral methyl group assists solubility (despite the lipophilicity increase), due to disruption of crystal packing. Moving from sulfonamide to amide derivatives also enhanced the hERG properties of the compounds (again, cf. **2a**, **2c** and **2e**). This finding was in accordance with the general trend for the piperazine series, that increased Log*D* led to a greater affinity for the hERG ion channel (Fig. 1).

Whilst introduction of a basic side chain in the amide series significantly increased solubility (cf. **2e** and **2g**), the compounds demonstrated low levels of exposure following oral dosing in rats and were not pursued further. In a related series of basic inhibitors, efflux had been shown to be the cause (data not shown). In contrast, the hydroxylated amides showed low levels of serum protein binding, and excellent oral exposure. To more fully understand the reasons behind the observed enzyme potency, we undertook structural studies to investigate the binding mode of the piperazines when bound to CDK2. The crystal structure of CDK2 complexed with **2e** is shown in Figure 2.

The hydrogen bonding interactions in the hinge region of CDK2 between Leu83 NH and the pyrimidine N, and between Leu 83 O and the aniline NH are preserved. However, a number of additional key features are visible. The tertiary amine nitrogen of the piperazine overlays on the sulfur atom of the corresponding sulfonamide analogues,[1] and interacts via a water molecule with the backbone

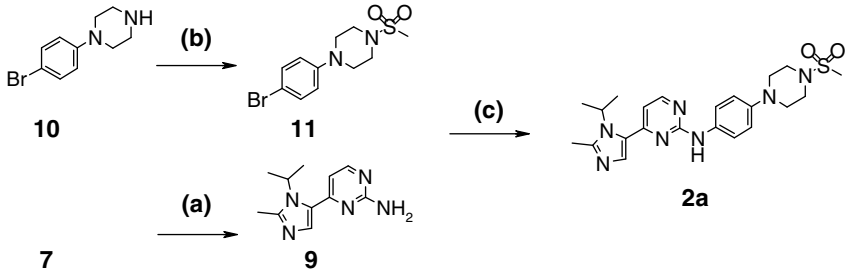

Scheme 3. Synthesis of piperazine **2a**. Reagents and conditions: (a) Guanidine hydrochloride, NaOMe, Butanol, reflux, 40%; (b) $MeSO_2Cl$, CH_2Cl_2, 80%; (c) $Pd_2(DBA)_3$, (2-(ditertbutylphosphino)biphenyl, NaO*t*Bu, 1,4-dioxane, 15%.

Table 2
Structures and in vitro activity for piperazines **2** and morpholines **12**

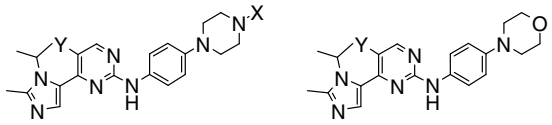

2 **12**

Compound	X	Y	CDK2 IC_{50} (μM)	MCF-7 IC_{50} (μM)	% Free (Rat)	hERG Mean IC_{50} (μM)	Solubility pH 7.4 (μM)	Log*D* pH 7.4	Oral DMPK AUC (μM h)[18]
2a	SO_2Me	H	<0.003	0.145	8	5.5	9	2.6	0.08
2c	$SO_2(CH_2)_2NMe_2$	H	0.003	<0.039	–	18	–	2.5	–
2d	$SO_2(CH_2)_2OMe$	H	<0.003	0.093	–	8.4	14	2.8	–
2e	$COCH_2OH$	H	0.017	0.17	22	>24	160	1.7	0.4
2f	$COCH(S\text{-}CH_3)OH$	H	0.017	0.22	–	>24	370	2.2	0.16
2g	$COCH_2NMe_2$	H	0.016	<0.027	40	>32	>3400	3.3	–
2h	$COCH_2NEt_2$	H	-	<0.022	–	–	>3700	–	0.0
2i	$COCH_2OH$	F	0.006	0.075	–	18	160	2.2	0.17
12a	–	H	0.009	0.29	–	–	56	2.9	0.16
12b	–	F	0.008	0.11	–	11	120	3.0	0.19

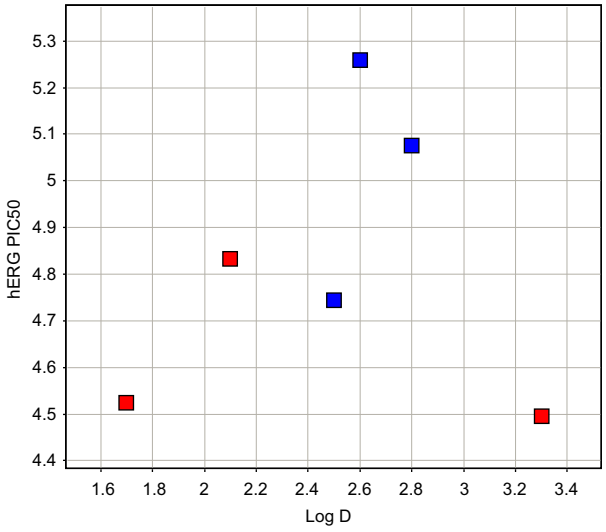

Figure 1. Log*D* versus IonWorks hERG pIC50; red, piperazine amides, blue, piperazine sulfonamides.

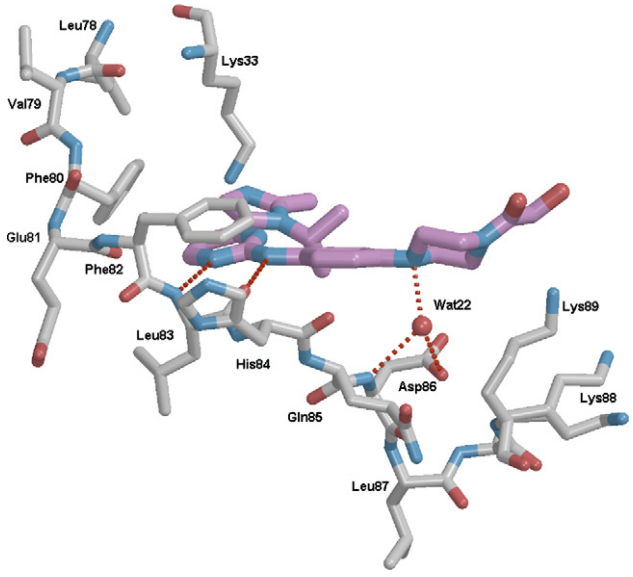

Figure 2. Crystal structure of CDK2 complexed with **2e**.[7] Selected nearby protein residues are shown. Hydrogen bonding interactions with the protein are indicated as dashed red lines. The figure was prepared using Bobscript and Raster3D.[8,9]

and side chain of Asp 86. This same interaction was observed in the crystal structure of an analogous imidazole sulfonamide complexed with CDK2, and helps to rationalise the selectivity that the piperazine series displays for this enzyme compared to other kinases. This is in accord with our previous observations that interactions with Asp86 confer an increase in CDK selectivity, and has been supported by selectivity testing in kinase screens (data not shown).[16] To explore further the nature and generality of this water-mediated contact, we elected to prepare further analogues that could potentially exploit a similar binding mode. Towards this goal, we targeted the morpholine **12a** (Table 2), prepared in an analogous fashion to intermediate **8**. Morpholine **12a** displayed cell activity and good physiochemical properties, in combination with higher in vivo clearance, higher lipophilicity and lower CDK potency than displayed by the piperazinyl amides. In an attempt to further investigate the SAR of the piperazinyl series, we next looked at substitution at the 5-position of the central pyrimidine ring. Whilst some substituents (not shown) proved beneficial from a potency and DMPK point of view, the effect on physical properties was, on the whole, significant with a reduction of aqueous solubility and an increase in plasma protein binding due to increased

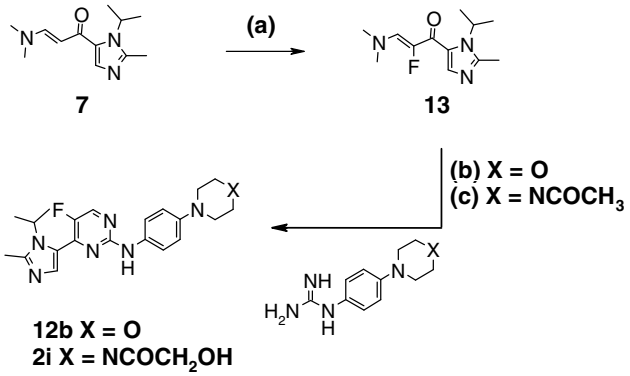

Scheme 4. Synthesis of 5-fluoro piperazines and morpholines **2i** and **12b**. Reagents and conditions: (a) Selectfluor, MeCN, 52%; (b) 2-methoxyethanol, 110 °C, 85%; (c) i—2-methoxyethanol, 110 °C, 83%; ii—IPA, concd HCl, 85 °C, 91%; iii—acetoxyacetyl chloride, Et_3N, CH_2Cl_2, RT, then 20% NH_3 in MeOH, RT, O/N 81% over two steps.

Table 3
Structures and in vitro activity for azetidine **14**, pyrrolidine **15** and proline amide **16**

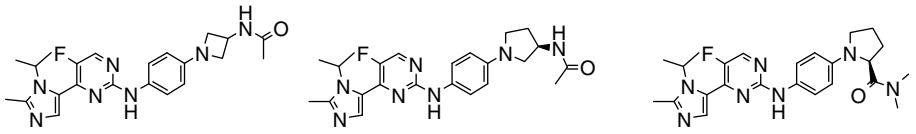

14 **15** **16**

Compound	CDK2 IC_{50} (μM)	MCF-7 IC_{50} (μM)	% Free (Rat)	Solubility (μM) pH 7.4	Log*D* pH 7.4
14	0.0005	—	5	120	2.8
15	>0.0003	0.14	—	9	3.3
16	0.046	—	—	—	—

Table 4
Structures and DMPK properties for piperazines **2e**, **2i** and morpholine **12b**

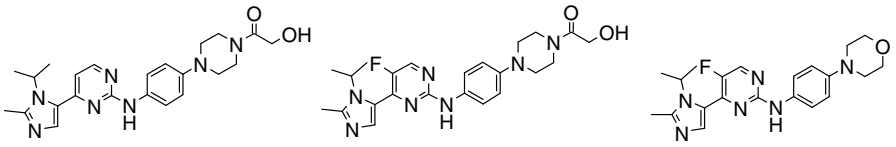

2e **2i** **12b**

Compound	Rat Vdss (L/Kg)	Rat Clp (ml/min/kg)	Rat bioavailability (%)	Dog Vdss (L/Kg)	Dog Clp (ml/min/Kg)	Dog bioavailability (%)
2e	2.5	15	59	3.4	19	79
2i	1.0	16	67	3.5	24	31
12b	1.3	26	34	2.9	140	3

Log*D*. Fluorination, in contrast, provides excellent gains in potency without the impact displayed by more lipophilic moieties. Fluorination of aminopropenone **7** was achieved using SelectFluor[17] in acetonitrile (Scheme 4) to give the product **13** as a golden crystalline solid.

Cyclisation as described above with a suitable guanidine delivered the fluorinated pyrimidine that could be further elaborated in an analogous fashion to the hydrogen pyrimidines (vide supra). The beneficial potency effect of the fluorinated compounds can be rationalised by the electronegative fluorine atom acidifying the aniline NH, and thereby increasing its hydrogen-bond donor strength to the hinge region of the protein. Gratifyingly, application of this SAR learning to the morpholine scaffold **12a** also led to noticeably more potent CDK inhibitors (e.g., **12b**, Table 2). A crystal structure of **12b** in complex with CDK2 confirmed the binding mode (data not shown), including retention of the water mediated contact. The results obtained for azetidine (**14**), pyrrolidine (**15**) and proline amide (**16**) templates (Table 3) are also consistent with the fluoro SAR leading to increased potency, and the water-mediated nitrogen contact giving CDK selectivity.

Encouraged by the evidence of oral exposure from rat cassette work, pleasing anti-proliferative cell potency and good physical properties of compounds **2e**, **2i** and **12b**, we next elected to undertake discrete rat and dog PK studies with these compounds. The results from this work are shown below in Table 4.

Whilst the two piperazine compounds **2e** and **2i** showed oral exposure in both rat and dog, it was apparent that the bioavailability of morpholine compound **12b** in the dog was limited by increased clearance relative to the rat. In view of these data, compounds **2e** and **2i** were subsequently evaluated for their ability to inhibit the growth of human SW620 xenografts in nude mice. Pleasingly, both compounds were shown to be active in this disease model with **2e** showing 80% tumour growth inhibition when dosed orally once a day at 7.5 mg/kg for 28 days. Compound **2i** showed 89% tumour growth inhibition when dosed orally once a day at 12.5 mg/kg for 28 days (Fig. 3).

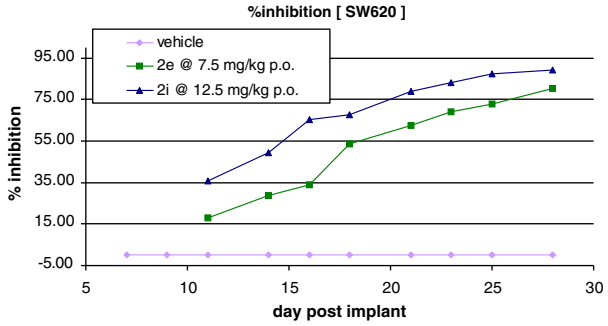

Figure 3. Inhibition of SW620 tumour xenografts in the nude mouse for compounds **2e** and **2i**. Compounds were dosed orally once a day for 28 days.

In summary, we have described a series of CDK inhibitors with a novel binding mode that exploits an unexpected interaction with Asp86, in an analogous but subtly different way to that displayed by the previously described sulfonamides. Two of these compounds have also been shown to inhibit in vivo tumour growth in clinically relevant disease models.

Acknowledgments

We acknowledge the excellent technical expertise of the following scientists: Kate F. Byth, Catherine Geh, Claire A. Brassington, Sandra E. Oakes, Malcolm Anderson, Stefan Gerhardt, Jon Read, Judith Stanway, Richard Fitzpatrick, Mike Walker, Sarah Kearney, Karoline Pitts and Sandra McGregor.

References and notes

1. Anderson, M.; Andrews, D. M.; Barker, A. J.; Brassington, C. A.; Breed. J.; Byth, K. F.; Culshaw, J. D.; Finlay, M. R. V.; Fisher, E.; Gingell, H. H. J.; Green, C. P.; Heaton, D. W.; Nash, I. A.; Newcombe, N. J.; Oakes, S. E.; Pauptit, R. A.; Roberts, A.; Stanway, J. J.; Thomas, A. P.; Tucker, J. A.; Weir, H. M. *Bioorg. Med. Chem. Lett.*, submitted for publication.

2. Thai, K.-M.; Ecker, G. F. *Bioorg. Med. Chem.* **2008**, *16*, 4107.
3. Schroeder, K.; Neagle, B.; Trezise, D. J.; Worley, J. *J. Biomol. Screening* **2003**, *8*, 50.
4. For recent reviews, see: (a) Yang, B. H.; Buchwald, S. L. *J. Organomet. Chem.* **1999**, *576*, 125; (b) Hartwig, J. F. *Angew. Chem., Int. Ed. Engl.* **1998**, *37*, 2046; (c) Wolfe, J. P.; Wagaw, S.; Marcoux, J.-F.; Buchwald, S. L. *Acc. Chem. Res.* **1998**, *31*, 805.
5. *NMR data for compound* **2e** *:* δ_H (300 MHz, DMSO-d_6) 1.38 (6H, d, J = 8.0 Hz), 2.46 (3H, s), 3.05 (4H, s), 3.48–3.60 (4H, m), 4.12 (2H d, J = 5.4 Hz), 4.57 (1H t, J = 5.5 Hz), 5.64–5.73 (1H, m), 6.91 (2H d, J = 8.9 Hz), 6.94 (1H, s), 7.38 (1H, s), 7.46 (2H d, J = 8.9 Hz), 8.30 (1H, d, J = 5.2 Hz), 9.16 (1H, s).
6. Inhibition of proliferation in whole cells was assayed using the Roche BrdU incorporation Elisa kit (Roche 1-647-229). MCF-7 cells were seeded into 96-well plates at 8×10^3 cells/well in DMEM (D6546) supplemented with 10% FCS and 1% Glutamine and allowed to adhere overnight. They were then treated with inhibitors for 48 h at 37 °C. Ten microlitres of BrdU labelling reagent were added to each well and plates were re-incubated at 37 °C for 2 h.Cells were fixed with 50 μl of FixDenat for 45 min, washed with wash buffer and then exposed to 75 μl of AntiBrdU POD for 90 min at RT.
   Cells were washed with wash buffer and 100 μl of TMB substrate was added to each well and plates were shaken vigorously for 10 min at RT. The reaction was stopped by the addition of 25 μl of 1 M H_2SO_4. Absorbance was then measured on a 96-well plate reader at 450 nm. The IC_{50} values for CDK inhibitors were determined by performing dose–response curves with individual compounds and determining the concentration of inhibitor producing fifty percent decrease in maximal signal. Cdk2/Cyclin E enzyme inhibition was screened using Spatial Proximity Assay radiometric technology (Amersham RPNQ0019 Protein A coated beads). The ability of Cdk2/E inhibitors to inhibit phosphorylation of the Retinoblastoma protein (gene region 792–928 expressed in a GST expression system and purified from *Escherichia coli*) by partially purified non-GST tagged CDK2/E (from a baculoviral insect cell lysate) was assessed. CDK2/E enzyme activity was titrated on a batch to batch basis. CDK2/E inhibitors were dissolved in 100% DMSO to 10 mM and diluted down in 5% DMSO to give a final concentration range of 10 to 0.003 μM.
   Ten microlitres of inhibitor were mixed with 25 μl of GST-Rb at 1.25 μg/well (XS), 400 nM cold ATP, +0.145 rmuCi [γ^{33}P]ATP Redivue (Amersham AH9968). Rb was stored at −80 °C in a buffer containing 50 mM Hepes, 10 mM $MnCl_2$, 1 mM DTT, 100 μM NaF, 100 μM NaVan, 10 mM NaGlycPhos, 5 μg/ml Aprotinin, 2.5 μg/ml Leupetin and 100 μM PMSF. Max wells had 10 μl of 5% DMSO and Min wells 10 μl of 10 μM final concentration Roscovitine (Calbiochem 557360).
   The reaction was started by the addition of 20 μl Cdk2/E (in a buffer containing 1 mg/ml BSA, 50 mM Hepes, 10 mM $MnCl_2$, 1 mM DTT, 100 μM NaVan, 100 μM NaF and 10 mM NaGlycPhos). Reaction volume was 55 μl. Plates were incubated at RT for 60 min. The reaction was stopped by the addition of 150 μl STOP solution containing 50 mM Hepes, 1:500 dilution of Anti-GST Ab (Molecular Probes A-5800), 0.5 M EDTA and Protein A-coated SPA beads (reconstituted in 25 ml of 50 mM Hepes). After 2 h incubation at RT, the plates were centrifuged at 2500 rpm for 5 min and then read on a TopCount NXT Microplate Scintillation Counter.
   The IC_{50} values for Cdk2 inhibitors were determined by performing dose–response curves with individual compounds and determining the concentration of inhibitor producing 50% decrease in maximal signal (diluent control).
7. Protein and crystals were obtained according to established procedures.[10,11] Diffraction data were collected on beamline PX14.2 at the SRS, Daresbury, at 100 K. Crystals were soaked in 5 mM compound **2e** overnight in mother liquor containing 10% DMSO. Data processing, data reduction and structure solution by molecular replacement were carried out using programs from the CCP4 suite.[12] Compound **2e** was modelled into the electron density using QUANTA.[13] The protein–compound complex model was refined using Refmac5,[14] and the final structure[15] has been deposited in the Protein Data Bank with the deposition code 2vv9 together with structure factors and detailed experimental conditions.
8. Esnouf, R. M. *J. Mol. Graph. Model.* **1997**, *15*, 132.
9. Merritt, E. A.; Murphy, M. E. P. *Acta Crystallogr.* **1994**, *D50*, 869.
10. Lawrie, A. M.; Noble, M. E.; Tunnah, P.; Brown, N. R.; Johnson, L. N.; Endicott, J. A. *Nat. Struct. Biol.* **1997**, *4*, 796.
11. Legraverend, M.; Tunnah, P.; Noble, M.; Ducrot, P.; Ludwig, O.; Grierson, D. S.; Leost, M.; Meijer, L.; Endicott, J. *J. Med. Chem.* **2000**, *43*, 1282.
12. CCP4, *Acta Crystallogr.* **1994**, *D50*, 760.
13. Quanta2000, Accelrys.
14. Refmac version 5.1.17, Murshudov, G. N.; Vagin, A. A.; Dodson, E. J. *Acta Crystallogr.* **1997**, *D53*, 240.
15. Crystallographic statistics for the CDK2-compound **2e** complex are as follows: space group $P2_12_12_1$, unit cell 53.2, 71.1, 71.9 Å, resolution 1.90 Å, 21,456 reflections from 57,306 observations give 97.3% completeness with R_{merge} of 4.0% and mean $I/\sigma(I)$ of 16.0. The final model containing 2206 protein, 152 water and 32 compound atoms has an R-factor of 19.1% (R_{free} using 5% of the data 22.7%). Mean temperature factors for the protein and the ligand are 37.9 and 33.4 Å^2, respectively.
16. Analysis of kinase protein sequences reveals only 34 kinases (including CDKs) having an Asp residue at this position. In a panel of 43 kinases, when tested at 10 μM, compound **2e** showed >90% inhibition against 10 enzymes. Similarly, compound **2i** showed >90% inhibition against six enzymes when tested at 10 μM against a panel of 24 kinases.
17. Nyffeler, P. T.; Duron, S. G.; Burkart, M. D.; Vincent, S. P.; Wong, C.-H. *Angew. Chem., Int. Ed.* **2005**, *44*, 192.
18. A cocktail of six compounds was formulated in propylene glycol using a combination of vortex mixing; sonication and high speed shear mixing. This formulation consisted of five test compounds (1 mg/ml) and a QC compound (0.5 mg/ml). The formulation was dosed (2 ml/kg) to two male rats (170–250 g) which had been fasted for ⩽16 h. The dose for the test compounds was 2 mg/kg and for the QC was 1 mg/kg. Serial blood samples were taken from rats at 0.5, 1, 2 and 4 h post-dose via the tail vein and a terminal sample was taken at 6 h post-dose. The blood samples were centrifuged and plasma was removed for analysis. The two plasma samples for a given time point were combined prior to analysis. A single set of six calibration standards containing all six compounds covering the concentration range (0.3 ng/ml–3 ug/ml) were prepared by spiking blank plasma. The samples and standards were extracted by precipitation with two volumes of acetonitrile followed by centrifugation. The resulting supernatant was then diluted with water (10-fold). The results obtained were used to determine the C_{max} (μM), AUC_{0-6h} (μM h) and t_{max} (h) for a given compound. All reported data are normalised to a dose of 1 μM/kg.